Nationaal Lucht- en Ruimtevaartlaboratorium
National Aerospace Laboratory NLR

NLR-TP-99104

Flow field investigations on a wing installed Counter Rotating Ultra-high-bypass Fan engine simulator in the low speed wind tunnel DNW-LST

G.H. Hegen, W. Puffert-Meissner, L. Dieterle and H. Vollmers

Nationaal Lucht- en Ruimtevaartlaboratorium

National Aerospace Laboratory NLR

NLR-TP-99104

Flow field investigations on a wing installed Counter Rotating Ultra-high-bypass Fan engine simulator in the low speed wind tunnel DNW-LST

G.H. Hegen, W. Puffert-Meissner*, L. Dieterle* and

H. Vollmers*

* *German Aerospace Research Centre (DLR)*

This report is based on an article to be presented at the 7th European Propulsion Forum on Aspects of Engine/Airframe Integration, 10-12 March 1999, Pau, France.

Division:	Aerodynamics
Issued:	5 March 1999
Classification of title:	Unclassified

Contents

3 Tables
10 Figures

(13 pages in total)

FLOW FIELD INVESTIGATIONS ON A WING INSTALLED COUNTER ROTATING ULTRA-HIGH-BYPASS FAN ENGINE SIMULATOR IN THE LOW SPEED WIND TUNNEL DNW-LST

G.H. Hegen

National Aerospace Laboratory (NLR), Emmeloord, The Netherlands

W. Puffert-Meissner

German Aerospace Research Centre (DLR), Braunschweig, Germany

L. Dieterle and H. Vollmers

German Aerospace Research Centre (DLR), Göttingen, Germany

ABSTRACT

For a better understanding of jet interference from wing mounted turbofan engines and for improved CFD modelling more detailed flow field studies and reliable test data are required. With this objective, within the framework of the DLR-NLR co-operation, flow field investigations have been carried out in the Low Speed wind Tunnel LST 3x2.25 m^2 of the DNW (German Dutch Wind tunnels) on a twin-jet transport aircraft half model (ALVAST).

The half model was tested in cruise configuration (clean wing without flaps) without and with a wing mounted engine simulator. Two types of engine simulators were used: a Through Flow Nacelle (TFN) and a turbo-powered Counter Rotating Ultra-high-bypass Fan (CRUF). All tests have been carried out at wind tunnel speed V_0=60 m/s (Mach number M_0=0.18). The flow fields behind the wing and engine simulators (TFN and CRUF) were investigated using a rake equipped with total pressure probes and a rake equipped with directional probes. In this way time-averaged flow field planes perpendicular to the tunnel flow were obtained. Non-intrusive flow field measurements were carried out using the Particle Image Velocimetry (PIV) technique. This technique was used to investigate the stream-wise development of the turbo-powered CRUF inlet and fan exhaust flow and the velocity flow field near wing and pylon. Information about both the unsteady and the time-averaged flow field was obtained.

The measurement techniques proved to be successful for engine/airframe interference studies. The two techniques are complementary and the results correspond well with each other. Furthermore a useful database has become available for further improvement of the CFD modelling. CFD computations have already been made for the cruise configuration without engine simulator, which correspond reasonably well with the five-hole rake measurements.

LIST OF SYMBOLS

b	wing span (=3.428 m)
c	local wing chord length
C_L	lift coefficient
C_D	drag coefficient
Cp_t	total pressure coefficient (=$(p_t-p_{to})/q_0$)
M	flow Mach number
M_0	tunnel free stream Mach number
p_t	local total pressure
p_{t0}	tunnel free stream total pressure
q_0	tunnel free stream dynamic pressure
RPM	CRUF rotational speed
U, V, W	model fixed flow velocity components
V_x,V_y,V_z	tunnel fixed flow velocity components
V_0	free-stream velocity in tunnel section
X, Y, Z	tunnel fixed coordinates (origin in model reference point) at α_m=0°)
α_m	model angle of attack (uncorrected for tunnel wall effects)

1. INTRODUCTION

Current testing techniques on engine-airframe integration deliver mainly test data on overall aerodynamic forces and surface pressure distributions. With this respect both DLR and NLR participated in the BRITE/EURAM programs DUPRIN (DUcted PRopfan INvestigations) and ENIFAIR (ENgine Integration for Future transport AIRcraft). Within these programs the engine-airframe interference effects are determined experimentally and theoretically (via CFD calculations) for a twin-jet transport aircraft model (ALVAST), supplied with different types of engine simulators. However, for a better understanding of the jet effects on the overall drag behaviour and for improved CFD modelling more detailed studies and reliable test data are needed. The influence of a jet on the flow field around an aircraft poses a very complex problem and requires detailed flow field visualisation to get insight into physics. NLR and DLR therefore decided to co-operate on some topics where further study was required (within the existing DLR-NLR co-operation

program: Low Speed Propulsion Airframe Integration).

Within this framework flow field investigations have been carried out in the DNW-LST on the ALVAST half model in cruise configuration. Since some of the flow field measurement techniques were used for the first time for engine/airframe interference studies, it was decided to restrict ourselves to the cruise configuration instead of the more realistic but also more complex high-lift configuration. Within phase 1 (October 1995, see Ref.1) the half model was tested without and with the Through Flow Nacelle (TFN), used for the simulation of the Counter Rotating Ultra-high-bypass Fan (CRUF) simulator. The flow field planes behind the wing and the TFN were investigated, using a rake equipped with five-hole probes and a rake equipped with total pressure probes. During phase 2 (November/ December 1996, see Ref.2) the half model was supplied with the turbo-powered CRUF simulator. The flow fields behind the wing and engine were not only investigated using the above mentioned rakes but also flow field measurements were carried out using the particle image velocimetry (PIV) technique. Emphasis of these tests was on the spatial development of the CRUF fan jet.

Additional CFD calculations for the cruise configuration, without engine simulator, at low speed conditions have been made by DLR.

2. EXPERIMENTAL SET-UP

2.1 Wind tunnel

The experiments have been performed in the Low Speed wind Tunnel (LST) of the DNW (German Dutch Wind tunnels). It is an atmospheric wind tunnel of the closed return circuit type with a free stream turbulence level of about 0.025%. The maximum velocity in the test section is about 80 m/s. The test section has a cross section of 3.00x2.25 m^2 and a length of 8.75 meters with excellent visual accessibility through removable transparent side panels. It is equipped with a remote controlled Y-Z traversing mechanism, allowing manual movements in axial X-direction over most of the test section length. All tests were carried out at a wind tunnel flow velocity of V_0=60 m/s (M_0=0.18).

2.2 Model

The ALVAST half model is the starboard side of the ALVAST complete model of the DLR (see Fig. 1). The ALVAST complete model is a twin engine model of approximately 3.5 meters span without tail, in cruise condition (no slat/flap) closely resembling an A320 aircraft 1:10 scale. Geometrical data and aerodynamic coefficients are given in tables 1 and 2 respectively. The ALVAST half model is provided with a pylon to mount one of the engine simulators (TFN or CRUF) to the wing. Both types of simulators are designed and owned by DLR (see Ref.3):

- The Through Flow Nacelle (TFN) (see also Fig.1) consists of an engine nacelle with internal diameter of 10” (254 mm). Enclosed in the nacelle is a through flow core with five inlet openings on its nose fairing.
- A technical drawing of the turbo-powered CRUF simulator is shown in Fig.2 and some main parameters are given in table 3. It has a two stage (8 blades per stage) counter-rotating fan of 10" (254 mm) diameter. This fan is driven by a four stage air turbine. The air turbine is driven by high-pressure air.

During the phase 1 test campaign the ALVAST half model (without and with TFN) was mounted in the DNW-LST from the top wall. During the phase 2 campaign, however, the model with turbo-powered CRUF simulator was mounted from the tunnel floor (see also Fig.3). In both cases a peniche is present between the model and the turntable of the DNW-LST to reduce influences of the tunnel boundary layer on the model. The peniche is mounted to the LST turntable while the model is mounted to an external balance system. The gap between the model and the peniche is closed by a labyrinth seal. An unintentional contact between the peniche and the model is detected electrically at two locations.

3. RAKE MEASUREMENTS

3.1 Devices for flow field measurements

The five-hole rake and the pitot rake have been used for flow field measurements behind the wing:

- The five-hole probe pressures are used for local flow vector and total pressure measurement. The five-hole rake is equipped with 18 five-hole probes with spherical heads (2.5 mm diameter). The individual probes are placed 15 mm apart (pitch), resulting in a rake span of 255 mm. The rake was calibrated at Mach numbers between M=0.07 and 1.2, and flow angles up to 45° .
- The pitot rake is used for total pressure measurement. It is equipped with 59 total pressure probes (1.1 mm diameter). The individual probes are placed 3.5 mm apart (pitch), resulting in a rake span of 203 mm.

The larger probe diameter could introduce a worse accuracy for the five-hole rake in a strong velocity

gradient. Therefore the pitot rake measurements are used for verification purposes.

The probe pressures are electronically scanned (with the electronically scanned pressure units placed inside the rake support sting) yielding high data rates and on-line pressure calibration abilities. The rake sting is mounted on a streamlined horizontal strut, which penetrates the wind tunnel side walls, and is fixed to the Y-Z traversing mechanism (see Fig.3). The rake is continuously traversed (traversing speed 3 mm/s) perpendicular to the wing span, while taking measurements about every second. The measurement grids of the five-hole rake and pitot rake are thus respectively $\Delta Y x \Delta Z = 15 x 3.4$ mm^2 and $3.5 x 3.4$ mm^2. For the five-hole rake it was decided to use a finer grid of $\Delta Y x \Delta Z = 7.5 x 3.4$ mm^2 for the complex flow field areas (wing tip and behind the simulators) by an intermediate traverse at half probe pitch. Dedicated data handling software and interpolation the calibration data base provides a nearly on-line presentation of measured data.

3.2 Test programme

For three model angles of attack α_m = 2°, 4° and 6°, flow field measurements have been made at two different positions behind the model (see also Fig.1):

I) At about half-chord distance behind the wing trailing edge.
II) At about one chord distance behind the wing trailing edge.

The following cruise configurations were tested:

- Clean wing without simulator.
- Clean wing with Through Flow Nacelle.
- Clean wing with turbo-powered CRUF. The rotational speed was set at RPM=3700 (idle) and 10500 rev/min (medium power).

Due to the cold turbine jet temperature (static temperature below 200K), the high power condition RPM=13300 rev/min could not be tested. The cold jet would cause freezing of the rake probes.

3.3 Results

Figure 4 shows a sample of the five-hole results at one chord distance behind the wing trailing edge (rake plane II) for the clean wing with turbo-powered CRUF simulator at RPM=3700 rev/min (idle condition) and α_m=4°. The cross flow velocity components are represented as arrows while the axial velocity components are represented as back ground colours. The wakes from the wing, wing tip and CRUF are clearly visible. Counter-clockwise cross flow components can be noted in the whole flow field and become stronger near the wing tip vortex. As may be expected over the complete half-span a down-wash of the wake exists with a stronger down-wash near the pylon. Furthermore, strong vortices are generated at the inboard side of the pylon and the outboard side of the nacelle. These vortices deform the originally circular nacelle wake to a square shape. All these effects increase in strength with angle of attack.

4. PARTICLE IMAGE VELOCIMETRY (PIV)

4.1 Experimental set-up

Two different PIV systems have been used: a photographic one for the investigation of the large-sized CRUF inlet flow and a digital one for studying the fan exhaust flow and the surrounding flow field near wing and pylon. Photographic films are still superior to digital cameras in so far as sensitivity and resolution are concerned. Consequently, they are capable to record larger observation areas than CCD cameras do. Over and above that, in the present application no additional technical efforts like image-shifting had to be made for photographic PIV because the structure of the inlet flow was expected to be very simple.

In both cases a frequency-doubled Nd:YAG laser system (wavelength 532 nm), consisting of two Q-switched oscillators, was employed for illumination. The laser system created double pulses of 2 x 300 mJ with a repetition rate of 10 Hz. A combination of spherical and cylindrical lenses spread the laser beam to a thin light sheet which entered the test section through a small opening in the wall and illuminated a plane inclined to the horizontal by 6° in Y-direction. An aerosol generator created oil droplets, 1 µm in size, by means of so-called *Laskin*-nozzles, see Ref.4. The tracer particles were released by a seeding rake inside the settling chamber of the wind tunnel.

Orthogonal to the light sheet, 100 mm lenses with an *f*-number 2.8 imaged the tracer particles by their scattered light at a working distance of about 2 meters. In the case of photographic recording the observation area was 0.4 x 0.6 m^2. A 35 mm SLR camera (Yashica) took 36 images per run on a b/w film Kodak T-max 3200 of 100 lines/mm resolution. For digital recording two CCD progressive scan cameras (Kodak) were used. They are able to take two single-exposed full frames (1024 x 1024 pixels) in quick succession each. The two cameras were triggered simultaneously and observed neighbouring areas (perpendicular to the

wing) of the same object plane, each 0.2 x 0.2 m^2 in size. In this configuration they took 2 x 30 image pairs per run. Additionally, the optical set-up, i.e. the laser light sheet and the cameras, could be shifted in X-direction in order to investigate the wake flow at three different distances from the engine simulator, resulting in 3 x 60 image pairs per run. The cameras were placed above the test section and mounted to the turntable, so that they did not need to be readjusted when changing the model angle of attack. The frame rate was always 10 Hz.

4.2 Test programme
Only the clean wing with turbo-powered CRUF has been tested. The measurement planes around the CRUF simulator are depicted in Fig. 5:

(a) Centre plane of the inlet (photographic PIV).
(b) Outboard plane behind the fan (digital PIV).

Two parameters varied: the rotational speed of the engine simulator (3700 rev/min, 10500 rev/min and 13300 rev/min) and the model angle of attack α_m (photographic PIV: 2° and 10°, digital PIV: 2°, 4° and 6°).

The photographs were evaluated by means of digital auto-correlation. To this end a scanner read in the negatives and digitalized the image data with a resolution of 2500 x 3700 pixels. The pictures taken with the CCD cameras were evaluated by means of digital cross-correlation (resulting in a spatial resolution of about 7 mm). For details of PIV image processing see Ref.5.

4.3 Results
In Figs. 6 and 7, results of the digital PIV measurements are presented. In Fig.6, a combination of six time-averaged velocity fields taken at RPM=3700 rev/min (idle condition) and α_m=4° are shown, and in Fig.7 the corresponding time-averaged vorticity field (one component, orthogonal to the measurement plane) of the same run is depicted.

In this case the jet coming out of the fan and the surrounding main flow have nearly the same velocity. The combined velocity field reveals the decelerated wake flow behind the fan cowling and the wing as well as the decelerated flow close to the stagnation point on the wing's leading edge. Additionally, areas of increased velocity can be seen below the wing and inside the adjacent jet. In this region the jet appears to be slightly deflected by the wing. This is confirmed by the vorticity field which indicates the velocity gradients of the wake.

5. CFD CALCULATIONS

5.1 Computational Method
Computations on the ALVAST cruise configuration (without engine simulator) were made with the FLOWer code, which is part of the MEGAFLOW software system at DLR, see Ref.6. The code is designed to simulate flows around complex aerodynamic configurations and solves the three-dimensional compressible Reynolds-averaged Navier-stokes equations in integral form in the subsonic, transonic and supersonic flow regime. Turbulence is modeled either by the algebraic model of Baldwin-Lomax or the more general two-equation k-ω transport model of Wilcox. In this case the k-ω turbulence model was used. The numerical procedure of FLOWer is based on a finite volume formulation on block-structured meshes. The numerical grid used for the calculations on the ALVAST-model was designed at NLR and improved in several steps (BRITE/EURAM program ENIFAIR).

For direct comparison with results obtained with the five-hole probes, additional numerical evaluations were necessary to obtain the flow field values in the same plane as measured by the five-hole probes.

5.2 Results
Fig.8 shows the computed tunnel fixed flow velocities at one chord length behind the wing trailing edge (rake plane II). As for the five-hole results, the axial velocity V_x is visualised by the background colours and the cross-flow velocities V_y and V_z are represented as arrows, allowing a direct comparison with the rake measurements.

6. DISCUSSION OF RESULTS
The CFD results of Fig.8 (without engine simulator) and the presented five-hole rake results of Fig.4 can be compared for the area well away from the simulator location. The cross velocity components agree very well but a systematic difference can be noted with respect to the axial velocity distribution. This difference is higher than the estimated five-hole rake measurement accuracy of ±0.01 (0.5 m/s) and is likely to be attributed to the tunnel wall effects (CFD calculations were made for a tunnel wall free condition).

Fig.9 shows the total pressure coefficient Cp_t distributions at about half chord distance (rake plane I) behind the turbo-powered CRUF for RPM=10500 rev/min and α_m=4°. At the left side the pitot rake and at the right side the five-hole rake results are presented. The Cp_t-values are represented as back ground colours and identical values are

connected via iso-lines. A good agreement between both rakes can be noted. The larger diameter of the five-hole rake probes does not result in systematic differences in the shear layers and vortex cores; only some extra scatter is introduced due to the calculation procedures (data base interpolation, etc.). Instead in the wing tip area the pitot rake shows a worse result than the five-hole rake (not shown here) due to the high local cross flow angles. The pitot rake measures only accurately for cross flow angles smaller than 20°.

The 2-D PIV and the five-hole rake results can be compared at the intersection line of both planes at about half chord distance (rake plane I) behind the turbo-powered CRUF (see also Fig.5). Therefore, the five-hole rake data (3-D) are projected on the body fixed 2-D PIV plane and two interpolated data sets have been used. In Fig.10 the body fixed axial and vertical velocity components U and W (or Mach number coefficients M_x/M_0 and M_z/M_0) are drawn versus height Z for α_m=4° and RPM=10500 rev/min. Shown by different colours are: the five-hole rake results, PIV single realisation and the mean of 30 PIV realisations. The deviations between the presented PIV realisations indicate that in the fan-jet (rotating flow) 30 realisations are probably not enough, to achieve a reliable mean. With exception of the lower fan-jet area, the mean PIV realisation shows a good agreement with the five-hole rake result. Both in the shear layer of the fan-jet and the wing wake, the differences are within 1 m/s (PIV and five-hole rake accuracies are respectively about 1 m/s and 0.5 m/s).

7. CONCLUDING REMARKS

The five-hole rake and PIV measurement techniques were successfully applied in the DNW-LST for engine/airframe interference flow field studies on the ALVAST half model in cruise configuration (no flaps). For this case the two techniques are complementary and the results correspond well with each other. Furthermore the precision of the five-hole rake data was verified by available pitot-rake data.

A more detailed analysis of this test will be required to reveal unsteady features of engine/airframe interference flow fields. Therefore advantage will be taken of the fact that instantaneous PIV measurement results are available.

Further analysis is underway at NLR with respect to the five-hole rake velocity fields along the model span. The data can be used to calculate the local viscous drag (total pressure losses), induced drag (vorticity) as well the lift. The local lift can be compared with the integrated wing pressure distributions while the total lift and drag can be compared with the measured balance forces.
A useful database with reliable data has become available for further improvement of the CFD modelling. CFD computations have already been made for the ALVAST cruise configuration without simulator, which correspond reasonably well with the five-hole rake measurements. Next, the ALVAST configuration with Through Flow Nacelle and turbo-powered CRUF simulator are to be computed. Preferably the wind tunnel walls are incorporated in the computations.

The DLR-NLR co-operation will continue with further analysis of the available PIV and five-hole rake data, and with the CFD computations. A wind tunnel test campaign on the (more realistic and also more complex) ALVAST half model in high-lift configuration equipped with the turbo-powered CRUF simulator, is planned in the DNW-NWB for May 1999. These tests will will include again five-hole rake, PIV and force measurements.

8. REFERENCES

1. Hegen, G.H., Test report of force and flow field measurements on the ALVAST half model in the Low Speed wind Tunnel LST Phase 1 -test number 5619-, TR 96576L.
2. Hegen, G.H., Test report of force and flow field measurements on the ALVAST half model supplied with turbo-powered CRUF simulator in the Low Speed wind Tunnel DNW-LST Phase 2 -test number 6628-, TR xxxxxL.
3. Hoheisel, H., The design of a Counter Rotating Ultra-high-bypass Fan simulator for wind tunnel investigation, DLR, Institut für Entwurfs-aerodynamik, Braunschweig, DLR-FB 93-20, March 1993.
4. Echols, W.H.; Young, J.A., Studies of portable air-operated aerosol generators, NLR (Naval Research Laboratory) Report 5929, Washington 1963.
5. Raffel, M.; Willert, C.E.; Kompenhans, J., Particle image velocimetry – a practical guide, Springer-Verlag, Berlin 1998.
6. Kroll, N.; Rossow, C.C.; Becker, K.; Thiele, F., MEGAFLOW - A Numerical Flow Simulation System. 21st ICAS congress, 1998, Melbourne, 13.09-18.09.1998, ICAS-98-2.7.4, 1998

connected via iso-lines. A good agreement between both rakes can be noted. The larger diameter of the five-hole rake probes does not result in systematic differences in the shear layers and vortex cores; only some extra scatter is introduced due to the calculation procedures (data base interpolation, etc.). Instead in the wing tip area the pitot rake shows a worse result than the five-hole rake (not shown here) due to the high local cross flow angles. The pitot rake measures only accurately for cross flow angles smaller than 20°.

The 2-D PIV and the five-hole rake results can be compared at the intersection line of both planes at about half chord distance (rake plane I) behind the turbo-powered CRUF (see also Fig.5). Therefore, the five-hole rake data (3-D) are projected on the body fixed 2-D PIV plane and two interpolated data sets have been used. In Fig.10 the body fixed axial and vertical velocity components U and W (or Mach number coefficients M_x/M_0 and M_z/M_0) are drawn versus height Z for α_m=4° and RPM=10500 rev/min. Shown by different colours are: the five-hole rake results, PIV single realisation and the mean of 30 PIV realisations. The deviations between the presented PIV realisations indicate that in the fan-jet (rotating flow) 30 realisations are probably not enough, to achieve a reliable mean. With exception of the lower fan-jet area, the mean PIV realisation shows a good agreement with the five-hole rake result. Both in the shear layer of the fan-jet and the wing wake, the differences are within 1 m/s (PIV and five-hole rake accuracies are respectively about 1 m/s and 0.5 m/s).

7. CONCLUDING REMARKS

The five-hole rake and PIV measurement techniques were successfully applied in the DNW-LST for engine/airframe interference flow field studies on the ALVAST half model in cruise configuration (no flaps). For this case the two techniques are complementary and the results correspond well with each other. Furthermore the precision of the five-hole rake data was verified by available pitot-rake data.

A more detailed analysis of this test will be required to reveal unsteady features of engine/airframe interference flow fields. Therefore advantage will be taken of the fact that instantaneous PIV measurement results are available.

Further analysis is underway at NLR with respect to the five-hole rake velocity fields along the model span. The data can be used to calculate the local viscous drag (total pressure losses), induced drag (vorticity) as well the lift. The local lift can be compared with the integrated wing pressure distributions while the total lift and drag can be compared with the measured balance forces.
A useful database with reliable data has become available for further improvement of the CFD modelling. CFD computations have already been made for the ALVAST cruise configuration without simulator, which correspond reasonably well with the five-hole rake measurements. Next, the ALVAST configuration with Through Flow Nacelle and turbo-powered CRUF simulator are to be computed. Preferably the wind tunnel walls are incorporated in the computations.

The DLR-NLR co-operation will continue with further analysis of the available PIV and five-hole rake data, and with the CFD computations. A wind tunnel test campaign on the (more realistic and also more complex) ALVAST half model in high-lift configuration equipped with the turbo-powered CRUF simulator, is planned in the DNW-NWB for May 1999. These tests will will include again five-hole rake, PIV and force measurements.

8. REFERENCES

1. Hegen, G.H., Test report of force and flow field measurements on the ALVAST half model in the Low Speed wind Tunnel LST Phase 1 -test number 5619-, TR 96576L.
2. Hegen, G.H., Test report of force and flow field measurements on the ALVAST half model supplied with turbo-powered CRUF simulator in the Low Speed wind Tunnel DNW-LST Phase 2 -test number 6628-, TR xxxxxL.
3. Hoheisel, H., The design of a Counter Rotating Ultra-high-bypass Fan simulator for wind tunnel investigation, DLR, Institut für Entwurfs-aerodynamik, Braunschweig, DLR-FB 93-20, March 1993.
4. Echols, W.H.; Young, J.A., Studies of portable air-operated aerosol generators, NLR (Naval Research Laboratory) Report 5929, Washington 1963.
5. Raffel, M.; Willert, C.E.; Kompenhans, J., Particle image velocimetry – a practical guide, Springer-Verlag, Berlin 1998.
6. Kroll, N.; Rossow, C.C.; Becker, K.; Thiele, F., MEGAFLOW - A Numerical Flow Simulation System. 21st ICAS congress, 1998, Melbourne, 13.09-18.09.1998, ICAS-98-2.7.4, 1998

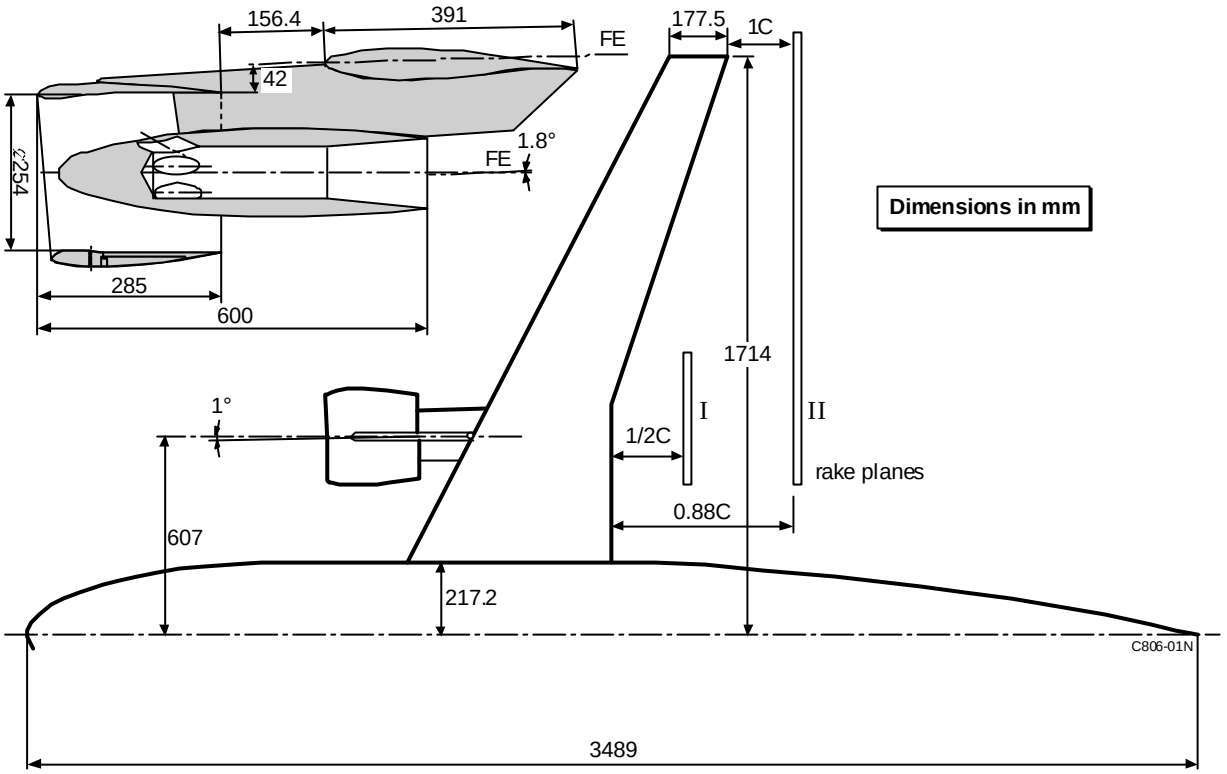

Fig. 1 ALVAST half model with simulator

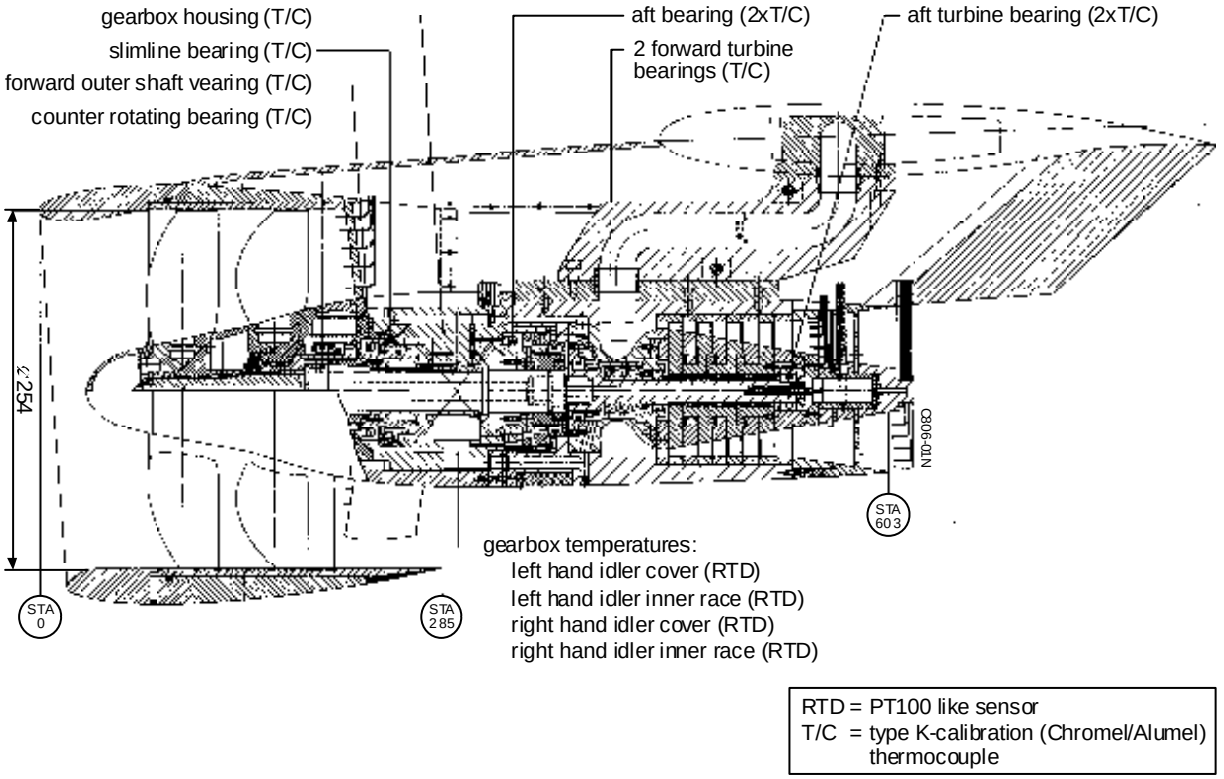

Fig. 2 Turbo-powered CRUF simulator

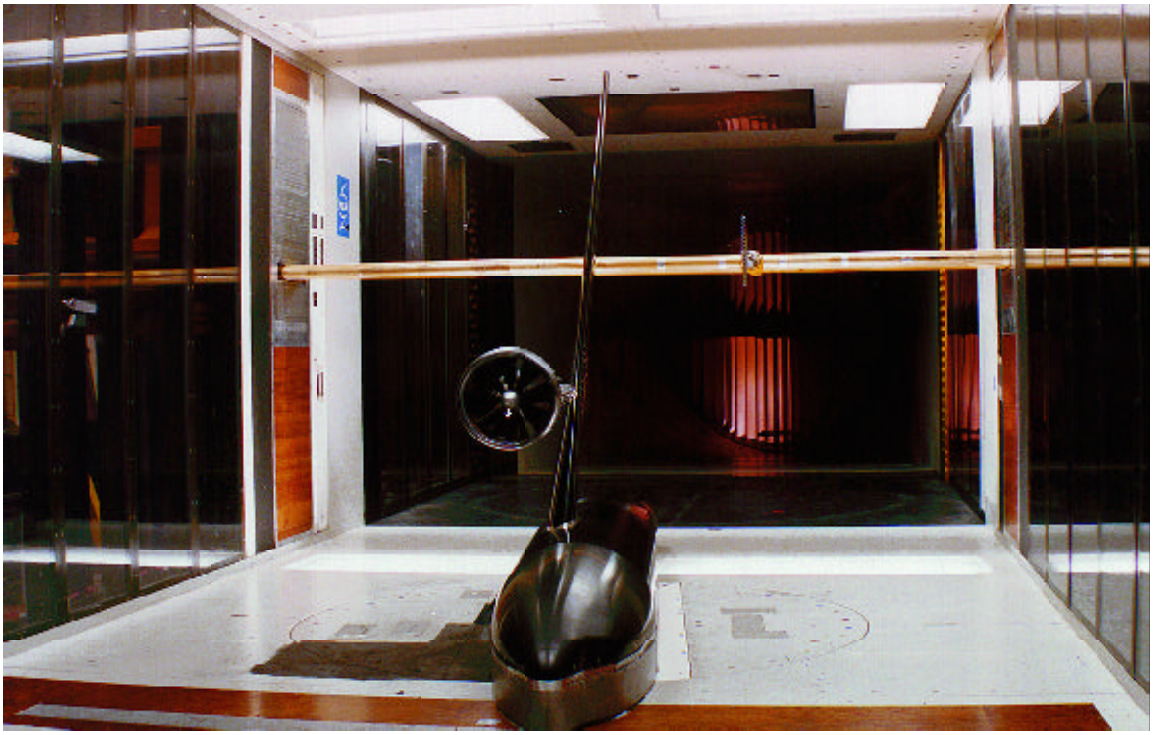

Fig. 3 ALVAST half model with turbo-powered CRUF simulator

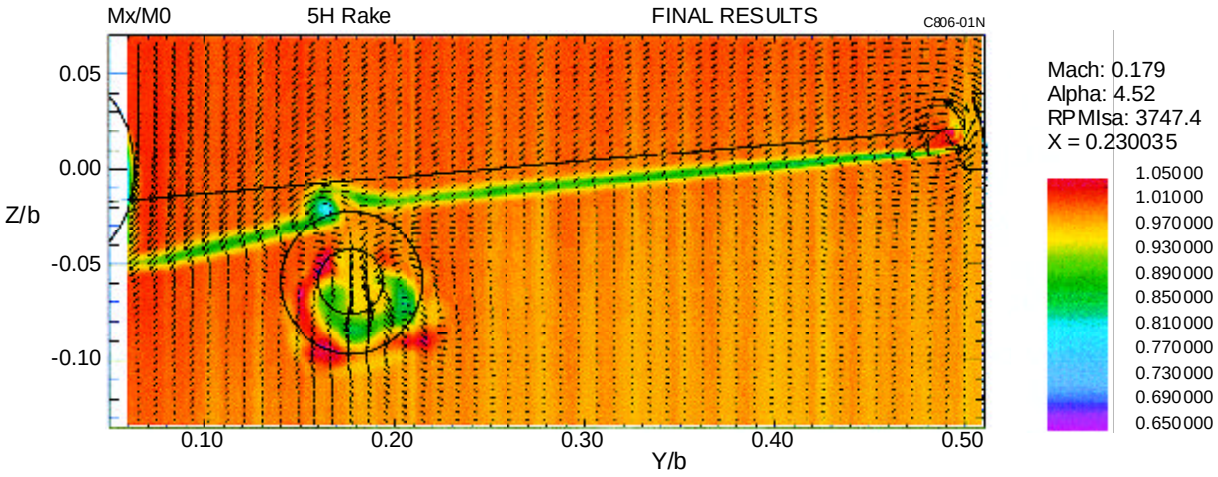

Fig. 4 Five-hole rake velocity plot at one chord distance (plane II) behind the ALVAST half model with turbo-powered CRUF simulator (α_m = 4° and RPM = 3700 rev/min)
Note: For reference the model discontinuities are indicated for α_m = 0°

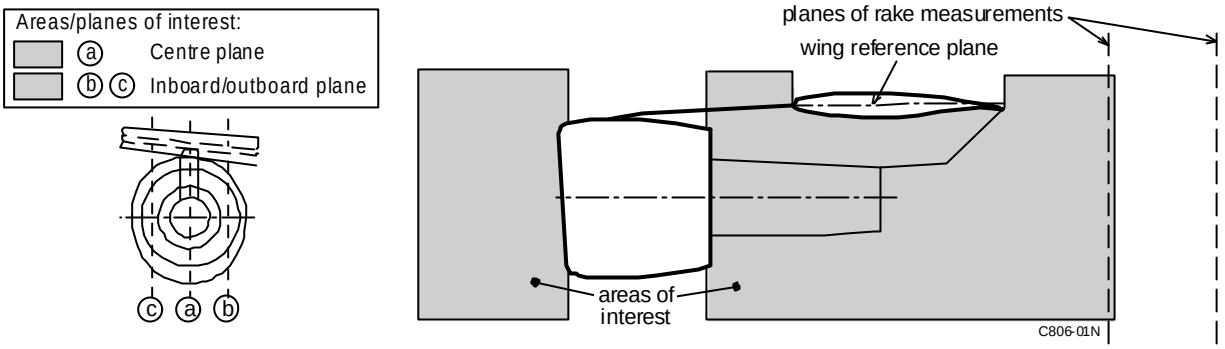

Fig. 5 PIV measurement planes around the turbo-powered CRUF simulator:
ⓐ Centre plane of the inlet (photographic PIV), ⓑ Outboard plane behind the fan (digital (PIV)

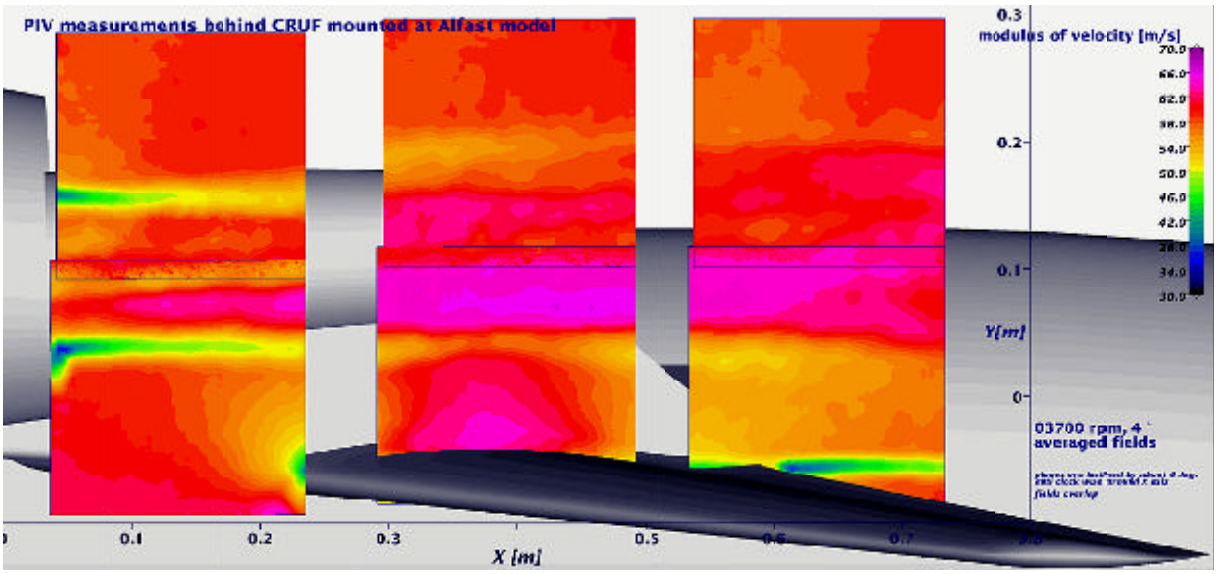

Fig. 6 Six time averaged velocity fields of the wake flow behind the turbo-powered CRUF simulator measured with digital PIV (α_m = 4° and RPM = 3700 rev/min)
Note: Inverted model

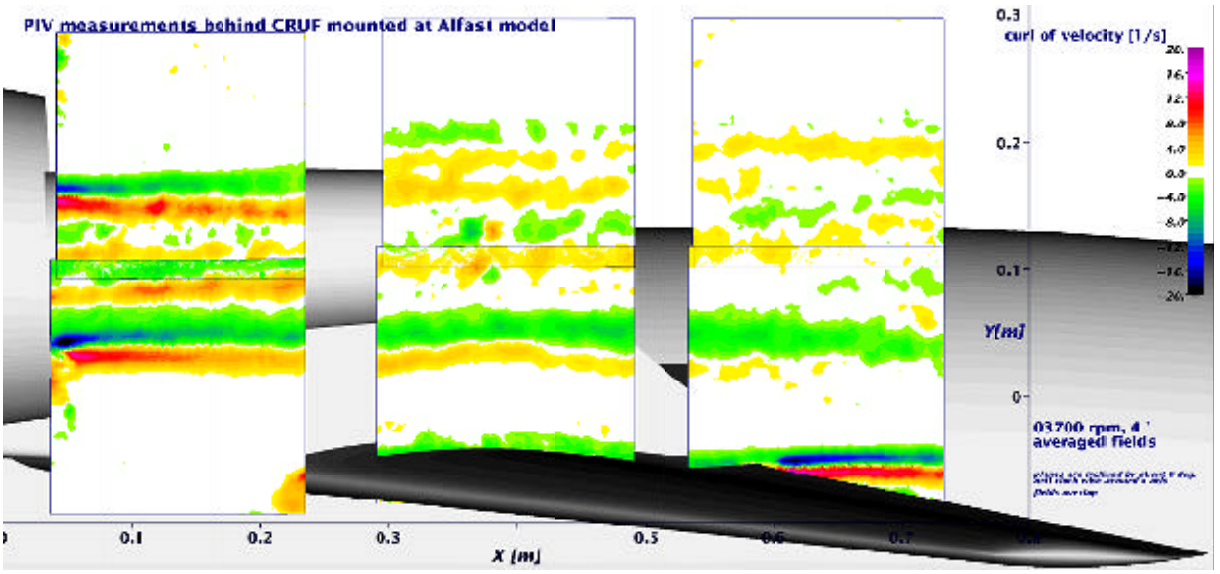

Fig. 7 Six time averaged vorticity fields of the wake flow behind the turbo-powered CRUF simulator measured with digital PIV (α_m = 4° and RPM = 3700 rev/min)
Note: Inverted model

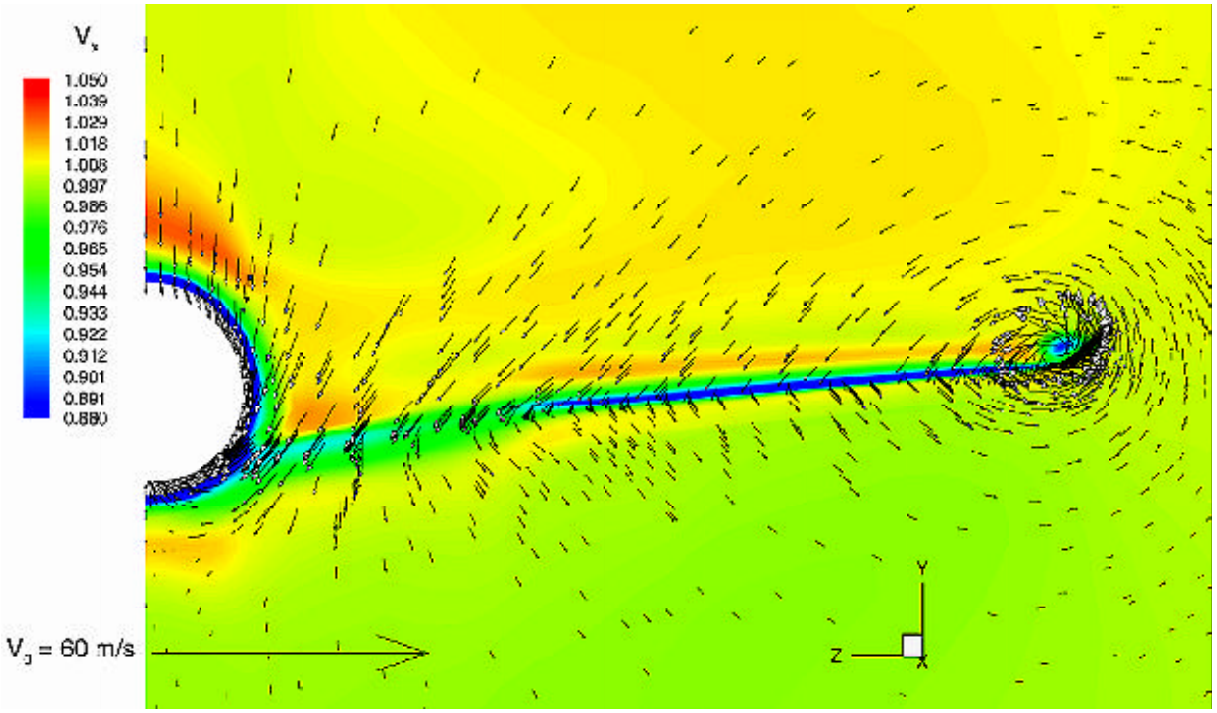

Fig. 8 CFD velocity plot at one chord distance (plane II) behind the ALVAST half model without simulator (α_m = 4°)

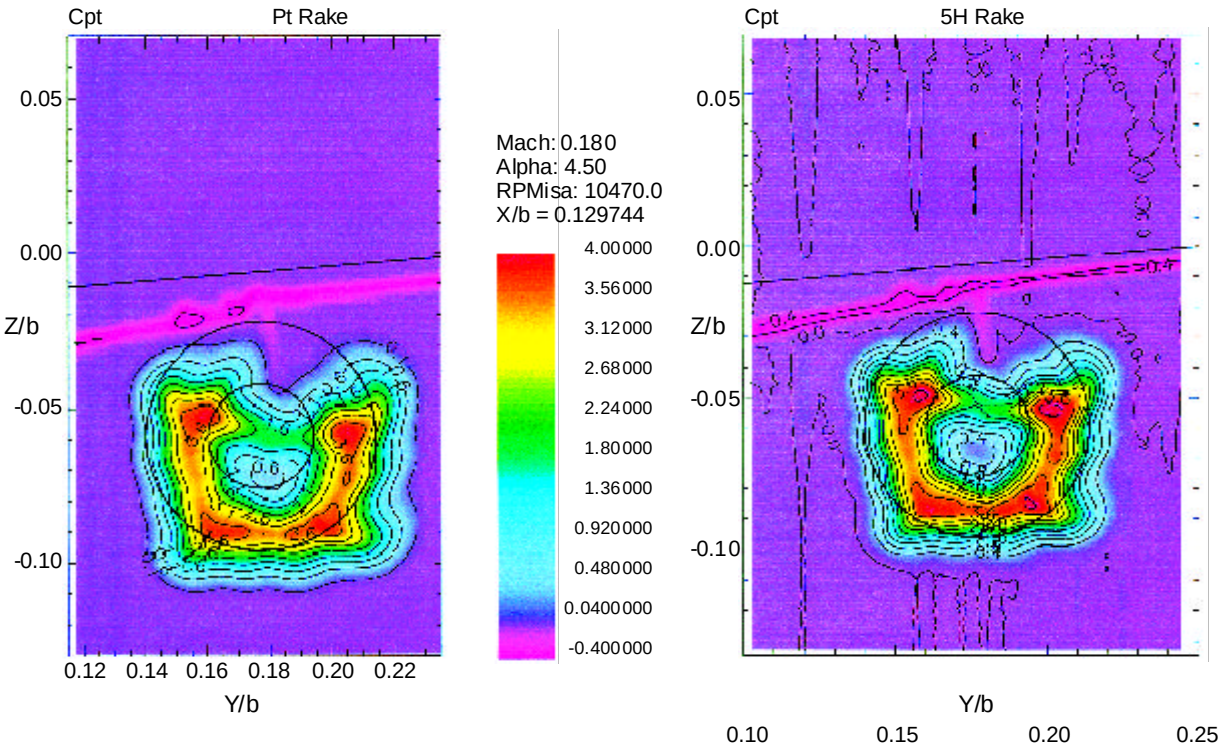

Fig. 9 Pitot-rake and five-hole rake total pressure coefficient distribution at half chord distance (plane I) behind turbo-powered CRUF simulator (α_m = 4° and RPM = 10500 rev/min)
Note: For reference the model discontinuities are indicated for α_m = 0°

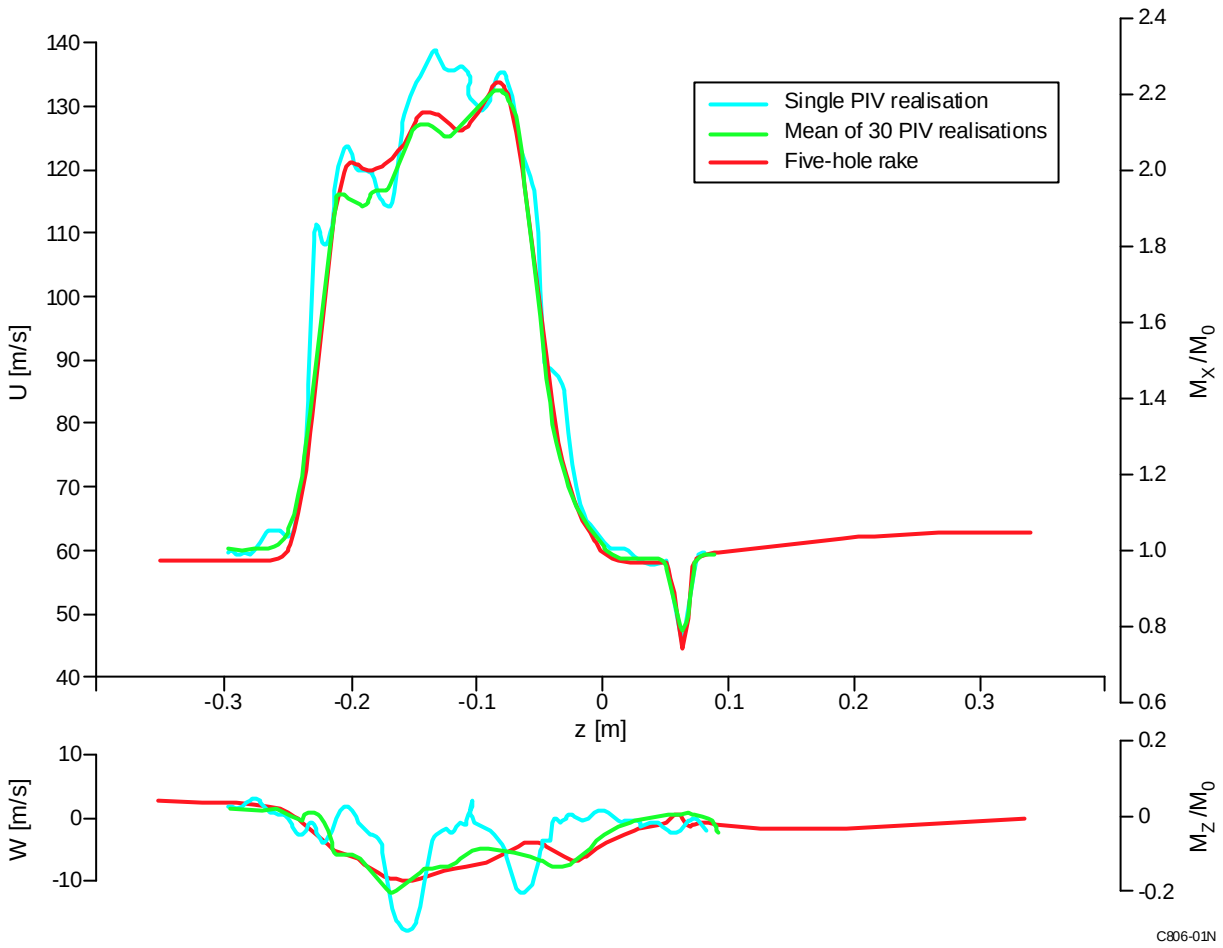

Fig. 10 Comparison of the projected five-hole rake and 2-D PIV results at the intersection line half chord distance (plane I) behind turbo-powered CRUF simulator (α_m = 4° and RPM = 10500 rev/min)